Redox Biology 36 (2020) 101659

Contents lists available at ScienceDirect

Redox Biology

journal homepage: www.elsevier.com/locate/redox

Research Paper

SERCA overexpression reduces reperfusion-mediated cardiac microvascular damage through inhibition of the calcium/MCU/mPTP/necroptosis signaling pathways

Chen Li [a,1], Qinghui Ma [b,1], Sam Toan [c], Jin Wang [d], Hao Zhou [d], Jianqiu Liang [a,*]

[a] Department of Cardiology, Foshan Hospital Affiliated with Southern Medical University (The Second People's Hospital of Foshan), Foshan, 528000, Guangdong, China
[b] Department of Oncology Hematology, Foshan Hospital Affiliated with Southern Medical University (The Second People's Hospital of Foshan), Foshan, 528000, Guangdong, China
[c] Department of Chemical Engineering, University of Minnesota-Duluth, Duluth, MN, 55812, USA
[d] Medical School of Chinese PLA, Chinese PLA General Hospital, Beijing, 100853, China

ARTICLE INFO

Keywords:
SERCA
Necroptosis
Cardiac microvascular I/R injury
Endothelial cells
Calcium

ABSTRACT

Endothelial cells lining the microvasculature are particularly vulnerable to the deleterious effects of cardiac ischemia/reperfusion (I/R) injury, a susceptibility that is partially mediated by dysregulated intracellular calcium signals. Sarco/endoplasmic reticulum Ca^{2+}-ATPase (SERCA) functions to recycle calcium from the cytosol back to the endoplasmic reticulum. The purpose of this study is to explore the roles and mechanisms of SERCA in protecting microcirculation against cardiac I/R injury. Our data showed that overexpression of SERCA significantly reduced I/R-induced luminal stenosis and vascular wall edema, possibly through normalization of the ratio between eNOS and ET-1. I/R-induced erythrocyte morphological changes in micro-vessels could be reversed by SERCA overexpression through transcriptional inhibition of the expression of adhesive factors. In addition, SERCA-sustained endothelial barrier integrity reduced the likelihood of inflammatory cells infiltrating the myocardium. Furthermore, we found that SERCA overexpression attenuated intracellular calcium overload, suppressed mitochondrial calcium uniporter (MCU) expression, and prevented the abnormal opening of mitochondrial permeability transition pores (mPTP) in I/R-treated cardiac microvascular endothelial cells (CMECs). Interestingly, the administration of calcium activator or MCU agonist induced endothelial necroptosis *in vitro* and thus abolished the microvascular protection afforded by SERCA in reperfused heart tissue *in vivo*. In conclusion, by using gene delivery strategies to specifically target SERCA *in vitro* and *in vivo*, we identify a potential novel pathway by which SERCA overexpression protects microcirculation against cardiac I/R injury in a manner dependent on the calcium/MCU/necroptosis pathway. These findings should be taken into consideration in the development of pharmacological strategies for therapeutic interventions against cardiac microvascular I/R injury.

1. Introduction

Coronary reperfusion strategies have been applied to reduce myocardial infarction–mediated cardiac damage by improving cardiomyocyte viability [1]. Although reperfusion strategies, such as primary percutaneous coronary intervention (PCI), create a complete recanalization of the occluded epicardial coronary arteries [2], effective myocardial reperfusion occurs in only about 50% of patients suffering myocardial infarction [3,4]. This phenomenon has been defined as ischemia-reperfusion (I/R) injury, and has been found to be an independent risk factor that predicts peri-operative mortality [5,6]. Significant efforts have focused on the identification and investigation of the mechanisms underlying cardiomyocyte I/R injury [7]. It is becoming increasingly clear that cardiomyocyte death, including apoptosis and necroptosis caused by oxidative stress and calcium overload, contributes to the development of cardiomyocyte I/R injury [8–11]. Many

* Corresponding author. Department of Cardiology, Foshan Hospital Affiliated with Southern Medical University (The Second People's Hospital of Foshan), Foshan, 528000, Guangdong, China.
E-mail address: 13415540346@126.com (J. Liang).
[1] Equal contribution.

https://doi.org/10.1016/j.redox.2020.101659
Received 25 April 2020; Received in revised form 6 July 2020; Accepted 21 July 2020
Available online 25 July 2020

cardioprotective drugs targeting cardiomyocyte survival have thus been introduced to patients during or before reperfusion strategies [12,13]. In contrast to cardiomyocytes, endothelial cell damage, termed "cardiac microvascular I/R injury" is a neglected topic [14,15]. The mechanism of I/R-mediated microvascular injury has not been described in detail.

Sarco/endoplasmic reticulum Ca^{2+}-ATPase (SERCA) recycles calcium from the cytosol back to the endoplasmic reticulum (ER) with the assistance of ATP [16]. Decreased SERCA expression and activity have been observed in cases of myocardial I/R injury and heart failure [17,18]. Pharmacological activation of SERCA is an effective way to alleviate cardiomyocyte damage through the normalization of calcium signals in cardiomyocytes [19,20]. Clinical studies [21,22] have confirmed the cardioprotective effects afforded by long-term upregulation of SERCA, which improves the ability of cardiomyocytes to contract and expand rapidly and regularly. Like cardiomyocytes, calcium homeostasis is critical for endothelial function [23]. Mild intracellular calcium overload induces endothelial spasm, whereas excessive intracellular calcium fluctuation promotes endothelial death [24,25]. However, the influence of SERCA on endothelial cell viability has not been fully explained. In addition, SERCA deficiency–mediated calcium imbalance has been identified as an upstream signal to induce cellular oxidative stress by modifying the activity of xanthine oxidase (XO) [26]. Considering the pathogenic roles played by oxidative stress and calcium overload in inducing cardiac I/R injury [27,28], we ask whether SERCA is a potential target for relieving cardiac microvascular I/R injury.

During cardiac I/R injury, two types of cell death have been reported: apoptosis and necroptosis [29,30]. Recent studies have found that necroptosis is the primary death pattern in these injuries [25,26]. It is conceivable that more than half of cardiomyocytes undergo necroptosis, whereas apoptosis accounts for only 30% of cardiomyocyte deaths [25,26]. Like apoptosis, necroptosis can be blocked by genetic or pharmacological strategies [31]. But it remains poorly understood how I/R injury–mediated endothelial necroptosis is governed. In reperfused cardiomyocytes, necroptosis is activated due to a rise in the expression of receptor-interacting protein 3 (Ripk3) which interacts with phosphoglycerate mutase 5 (PGAM5) and then induces mixed-lineage kinase-domain–like pseudokinase (MLKL) phosphorylation and mitochondrial permeability transition-pore (mPTP) opening [32,33]. Subsequently, MLKL migrates onto intracellular bio-membranes including the mitochondrial membrane, ER membrane, lysosome membrane, and cell membrane [34]. After localization onto the lipid bilayer, MLKL promotes the formation of pores across the membrane, leading to the swelling and rupture of organelles or cytoplasm [35,36]. In addition, mPTP-mediated ATP depletion is a feature of necroptosis [37]. Although Ripk3 upregulation, PGAM5 activation, and mPTP opening have been observed in the context of cardiac microvascular I/R injury [25,26], the downstream events and molecular alterations in endothelial cells have not been identified. In light of the link between ER membrane damage and SERCA downregulation, we ask whether SERCA inactivation is implicated in the transduction and amplification of the necroptosis signal. The overall aim of this experiment is to understand the action of SERCA on endothelial necroptosis during cardiac microvascular I/R injury.

2. Methods

2.1. AAV9-mediated SERCA overexpression

Adeno-associated virus-9 (AAV9) genome particles were obtained from Vector Gene Technology. Mouse SERCA was cloned into AAV9 vectors, which were injected subcutaneously into neonatal mice at the nape of the neck, at a titer of 0.5×10^{11} vector genomes per gram of body weight (vg/g). Control AAV9 vectors were injected at the same dosage and time points. After 8 weeks, heart tissues were collected, and the overexpression efficiency was measured through western blots (data not shown). *In vitro*, SERCA AAV9 were transfected into CMECs, as previously described [38]. The overexpression efficiency was measured through western blots (data not shown).

2.2. Cardiac ischemia/reperfusion (I/R) injury model

Cardiac I/R was surgically induced as described previously [39]. In brief, male C57BL/6J mice (8–12 weeks of age, 20–25 g) received AAV9 SERCA ($SERCA^{AAV9}$ group) or control AAV9 vectors (control group). These mice were anesthetized with pentobarbital sodium (60 mg/kg) and ventilated with a rodent ventilator. The left anterior descending coronary artery was ligated with a 6–0 silk suture, and ischemic damage was confirmed by observation of the blanching of the myocardium in the affected area. After 45 min of ischemia, reperfusion was achieved in the left anterior descending coronary artery for about 4 h. Animals in the sham group underwent all surgical procedures for I/R induction except the ligation step. The I/R model and treatment were performed by a single experienced operator under blinded conditions. To induce intracellular calcium overload, a single intraperitoneal (i.p.) injection of ionomycin at 1 mg/kg was used 30 min before the I/R model. In addition, to activate MCU in $SERCA^{AAV9}$ mice, spermine i.p. treatment at 5 mg/kg was used 60 min before I/R surgery. Dead mice and mice with no decrease in heart function at baseline were excluded. Completely randomized design and blinding were adopted in the animal experiments.

2.3. Heart histology

The heart tissue was perfused free of blood with cold PBS and fixed with 10% buffered formalin after the trachea was cannulated [40]. All the tissues were held under a pressure of 15 cm H_2O and preserved for 24–48 h in 10% buffered formalin. Formalin-fixed tissues were washed with PBS and dehydrated in 70% ethanol followed by paraffin processing. The samples were cut into 4- to 5-μm–thick sections, stained with H&E, and determined by light microscopy [41].

2.4. Cardiac microvascular endothelial cell (CMEC) culture and treatment

CMECs were isolated from mice as previously described [42]. Primary CMECs were cultured in a vascular cell basal medium supplemented with endothelial cell growth kit VEGF, 2% FBS, 100 U/ml penicillin, and 100 μg/ml streptomycin (endothelial cell growth medium). Cells were cultured at 37 °C in an atmosphere of 5% CO_2 and 95% air. The purity of the cells was confirmed by the cobblestone morphology and vWF immunocytochemical staining (data not shown). Hypoxia/reoxygenation (H/R) injury was caused through 30 min of hypoxia and 2 h of reoxygenation. $[Ca^{2+}]i$ activator (ionomycin, 3 μM for 2 h) and MCU agonist (spermine, 10 μM for 2 h) were administrated into SERCA-overexpressed CMECs to offset the regulatory effects afforded by SERCA on calcium homeostasis and MCU inhibition.

2.5. Immunoblotting analysis

Reperfused hearts tissues and cultured CMECs were washed twice with ice-cold PBS and harvested in RIPA Lysis and Extraction Buffer (Life Technologies), Halt Protease Inhibitor Cocktail (Life Technologies), and Halt Phosphatase Inhibitor Cocktail (Life Technologies). A Pierce BCA Protein Assay Kit (Life Technologies) was used for the colorimetric detection and quantitation of total protein [43]. A total of 25 μg of protein was separated on 4%–12% Tris-Glycine Mini Gels (Life Technologies) and transferred to PVDF membranes (Merck Millipore). The membranes were probed with antibodies to SERCA (1:1111, Abcam, #ab150435), MCU (1:1000, Cell Signaling Technology, #14997), *p*-eNOS (Ser1117) (1:1000, Abcam, #ab184154), ET-1 (1:1000, Abcam, #ab2786), and GAPDH (1:5000) (MilliporeSigma, cat# ABS16). Protein signals were detected using horseradish peroxidase (HRP)–conjugated secondary antibodies and enhanced chemiluminescence (ECL) western

blotting detection reagents (Thermo Fisher Scientific, MA, USA) [44].

2.6. Immunofluorescence

Immunofluorescence was performed as previously described [45]. Samples were fixed with 4% paraformaldehyde for 10 min, washed 3 times with 100 mmol/L glycine in HBSS for 10 min, and washed once with HBSS for 10 min [46]. Then the samples were permeabilized with 0.2% Triton X-100 in PBS for 10 min, blocked with 5% donkey serum for 1 h at room temperature, and incubated with Gr1 (1:1000, Abcam, #ab25377) and troponin T (1:1000, Abcam, #ab ab8295) overnight at 4 °C. After being washed 4 times, the cells were incubated by with donkey anti-mouse 488 (Invitrogen, A-21202) and donkey anti-rabbit 594 (Invitrogen, A-21207) secondary antibodies for 1 h at room temperature. The cells were then rinsed 4 times and mounted on glass slides using Vectashield mounting medium (Vector, H-1500) containing DAPI [47]. Intracellular calcium ($[Ca^{2+}]i$) and mitochondrial calcium ($[Ca^{2+}]m$) were stained using Furo-2AM (Molecular Probes) and Rhod-2 (Molecular Probes), respectively, as previously described [23].

For the immunohistochemistry of the heart, the tissues were embedded in paraffin, sectioned, and mounted to the slides. All the slides were rehydrated with xylene and decreasing concentrations of ethanol, and then antigen retrieval was performed using sodium citrate buffer [48]. After extensive washing with PBST, the slides were incubated with secondary antibody for 1 h and mounted with Vectashield containing DAPI. Confocal images were acquired with a laser-scanning confocal microscope (Zeiss LSM 510 META) using Hg lamp and UV-filter set to detect DAPI (band pass (BP) 385–470 nm emission), 488 nm excitation laser line to Alexa 488 (BP505–-550 nm emission), and 568 nm excitation laser line to Alexa Fluor 568 (excitation/emission ~578/603 nm).

2.7. Quantitative real-time RT-PCR analysis

Total RNA was isolated using Trizol (Invitrogen Life Technologies). Following reverse transcription with a High-Capacity cDNA Reverse Transcription Kit (Applied Biosystems), quantitative real-time PCR analysis was performed using an ABI 7500 system with Brilliant II SYBR Green QPCR Master Mix (Agilent) [49]. The primers used for analysis were as follows: MCP1 (forward, 5′GGATGGATTGCACAGCCATT-3’; reverse, 5′-GCGCCGACTCAGAGGTGT-3′), IL1 (forward prime, 5′-TTGCTCGAGTGAGTGAGGAT-3′; reverse prime 5′-TGTGACAGC GATGGACAGTG-3′), GAPDH, 5′-CCCAATGTGTCCGTCGTGGAT-3′ and 5′TGTAGCCCAAGATGCCCTTCAG-3’. The data were presented as the fold change relative to control [50].

2.8. Endothelial cell barrier function

Endothelial cell barrier function was measured through FITC-dextran assay and TER experiment. After treatment, 150 μl of culture medium containing FITC-dextran was added to each insert, and 500 μl of growth medium without FITC-dextran was added to each receiver plate well. The FITC-dextran was allowed to permeate through the monolayer, and levels of FITC-dextran were measured in the receiver chamber over 3 h. Every 30 min, 100 μl of medium was collected from the receiver well and replaced with an equal volume of fresh medium. Permeability was quantified by fluorescent intensity (of FITC-dextran) on a plate reader (SpectraMax M5, Molecular Devices) via fluorescence at 485 nm excitation and 535 nm emission wavelengths in a time-dependent fashion. The TER experiment was conducted using an In Vitro Vascular Permeability Assay Kit (ECM640, Millipore, USA) in accordance with the manufacturer’s manual.

2.9. LDH cytotoxicity experiment, TUNEL staining, and mPTP opening assay

LDH release assay was performed through an LDH Cytotoxicity Assay Kit (Beyotime, China, Cat. No:C0016) [51]. For TUNEL staining, cells were incubated with In Situ Cell Death Detection kit (Roche). Subsequently, the number of TUNEL–positive cells was observed and analyzed using a fluorescence microscope [52]. The mPTP opening rate was determined as previously described [53]. In brief, 2 μL of a calcein AM working solution was incubated with cultured CMECs for 30 min in the dark at 37 °C [54]. After being washed with PBS, the samples were measure using a microplate reader set to a wavelength of 450 nm (Epoch 2; BioTek Instruments, Inc.) [55].

2.10. Statistical analysis

All data were reported as Mean ± SE. Comparisons among three or more groups were evaluated for significance ($p < .05$) through one-way analysis of variance (ANOVA) followed by Bonferroni’s multiple comparison test, and comparisons among groups after multiple treatments were evaluated through two-way ANOVA followed by Bonferroni’s multiple comparison test. P values of less than 0.05 were considered statistically significant. Statistical calculations were carried out using GraphPad Prism 6.0.

3. Results

3.1. SERCA overexpression reduces I/R-caused cardiac microvascular damage

To identify the alterations of SERCA in response to cardiac microvascular I/R injury, protein analysis using western blots was performed. Relative to the sham-operated control group, I/R injury significantly reduced the expression (Fig. 1A and B) and activity (Fig. 1C) of SERCA in the heart. To investigate of the role of decreased SERCA in microvascular damage, AAV9 SERCA was delivered into the heart tissues before I/R injury. Then microvascular structure and function were observed. Histopathological assessment of cardiac microcirculation using an electron microscope (EM) revealed more luminal stenosis, vascular wall edema, or endothelial prolapse in mice subjected to I/R than in the sham-operated control group (Fig. 1D). Interestingly, AAV9 SERCA administration reduced microvascular damage caused by I/R injury quite obviously, as shown by the augmented lumen diameter. Due to a narrowed lumen, histological analysis by H&E staining revealed markedly increased erythrocyte aggregation in I/R-treated mice over the sham mice (Fig. 1E). In addition, we found a sword-shaped erythrocyte in untreated mice but a sphere of erythrocyte in I/R-treated mice (Fig. 1E), suggesting that I/R induced a hydrodynamic change around the erythrocyte due to microvascular damage. Consistently with the EM data, mice treated with AAV9 SERCA showed significant reduction of erythrocyte aggregation (Fig. 1E), which was followed by a normalization of erythrocyte morphology in the presence of I/R injury.

Microvascular relaxation and contraction depend on endothelium-generated eNOS, a powerful vascular relaxing factor [14]. Western blot analysis demonstrated a drop in eNOS phosphorylation in I/R-treated mice relative to the control mice (Fig. 1F–H). In addition, the levels of vascular constriction factors such as ET-1 were significantly upregulated by I/R injury relative to the untreated mice (Fig. 1F–H). However, SERCA overexpression significantly upregulated eNOS phosphorylation and downregulated the expression of ET-1 in hearts suffering from I/R injury (Fig. 1F–H).

Normal microvascular prevents inflammatory cells from invading from the blood into the myocardial tissue [4]. Increased inflammation response in the myocardium is another feature of microvascular injury. Immunofluorescence assay revealed an increase in the expression of Gr1-positive neutrophils in the myocardium of I/R-treated mice, as

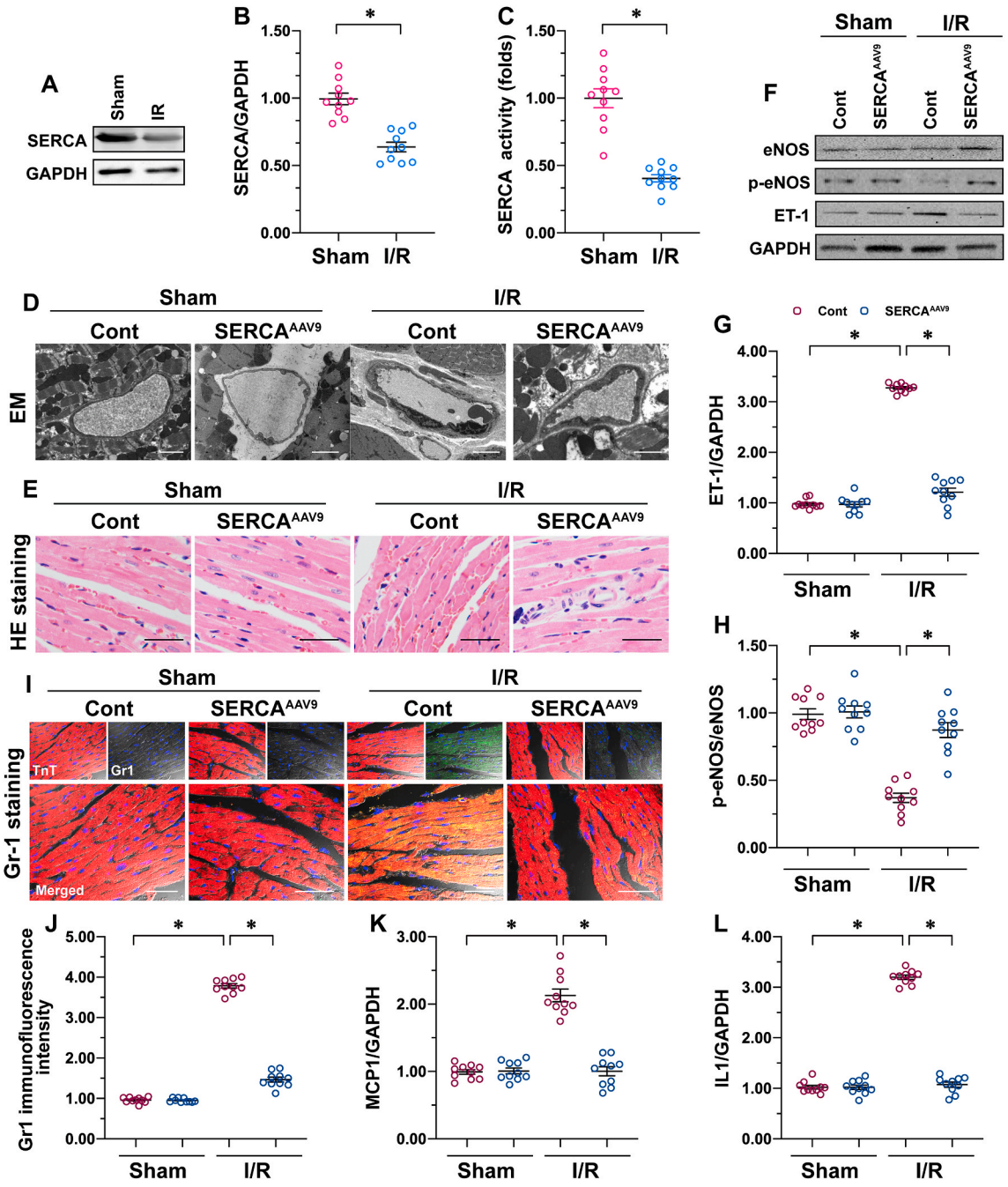

Fig. 1. SERCA overexpression reduces I/R-caused cardiac microvascular damage. Male C57BL/6J mice received AAV9 SERCA (SERCA^{AAV9} group) or control AAV9 vectors (control group) before I/R injury. An I/R injury model was induced through 45 min of ischemia and 4 h of reperfusion. Animals in the sham group underwent all surgical procedures for I/R induction except the ligation step. **A–B.** Proteins were isolated from reperfused hearts, and then the levels of SERCA were measured through western blots. **C.** ELISA assay for SERCA activity. **D.** Cardiac microcirculation was observed using an electron microscope (EM). **E.** H&E staining to detect erythrocyte aggregation. **F–H.** Proteins were isolated from reperfused hearts, and then the levels of phosphorylated eNOS and ET-1 were measured through western blots. **I–J.** Immunofluorescence for Gr-1 in a reperfused heart. The relative immunofluorescence intensity of Gr-1 was detected with Image-J software. **K–L.** RNA was isolated from reperfused hearts, and the transcriptions of MCP1 and IL-1 were determined through qPCR. *p < .05.

compared to the control mice (Fig. 1I and J). A qPCR analysis of inflammation cytokines further confirmed an agitated inflammation response in I/R-treated mice (Fig. 1K–L). Interestingly, SERCA overexpression was associated with a drop in the immunofluorescence signals of Gr1-positive neutrophils in the myocardium (Fig. 1I and J), accompanied by decreased inflammation factor transcription in the presence of I/R injury (Fig. 1K–L). Overall, I/R-mediated cardiac microvascular damage can be attenuated by SERCA overexpression.

3.2. SERCA overexpression improves endothelial function under H/R conditions

To clarify the molecular mechanisms underlying SERCA-mediated microvascular protection, cardiac microvascular endothelial cells (CMECs) were isolated from mice and transfected with AAV9 SERCA before undergoing hypoxia-reoxygenation (H/R) stress *in vitro*. Consistently with *in vivo* observations, H/R stress reduced eNOS phosphorylation and augmented ET1 expression in CMECs more than in the control

group (Fig. 2A–C). Interestingly, SERCA overexpression reversed the balance between eNOS phosphorylation and ET1 expression (Fig. 2A–C), indicating an essential role for SERCA in the regulation of endothelium-dependent vascular relaxation. Erythrocyte aggregation or hemodynamic alteration might be a consequence of the increased expression of adhesion molecules, which elevate the likelihood of thrombogenesis. Using qPCR, we were able to visualize an increase in the transcription of ICAM1 and VCAM1 (Fig. 2D and E), two critical adhesive factors expressed on the surface of the endothelium. However, in SERCA-overexpression CMECs, both ICAM1 and VCAM1 were transcriptionally downregulated (Fig. 2D and E) through an unclear mechanism.

In addition to expressing adhesion molecules, the endothelial barrier is an indispensable factor in thrombogenesis and inflammation-cell infiltration. To analyze alterations in the endothelial barrier's functioning and integrity, we applied a FITC-dextran clearance assay and an TER assay. Increased endothelial permeability was associated with an elevation in the concentration of remaining FITC-dextran, whereas decreased intercellular junction results in decreased ionic conductance (TER assay) of endothelial cells [39]. After exposure to H/R injury, the remaining FITC-dextran increased, whereas the TER value was reduced in CMECs (Fig. 2F and G); this alteration could be corrected by SERCA overexpression. Therefore, the above data confirm that endothelial function can be normalized by SERCA in the presence of H/R injury *in vitro*.

3.3. Necroptosis and apoptosis can be reduced by SERCA

I/R induces apoptosis and necroptosis in cardiomyocytes, but this finding is not repeated in CMECs. In our study, an LDH cytotoxicity assay demonstrated that H/R treatment causes more LDH to be released into the medium than in the control group (Fig. 3A), an indicator of endothelial cell membrane rupture. In parallel to these data, TUNEL assay was used to confirm an increase in the endothelial death index upon H/R exposure (Fig. 3B and C). Of note, in CMECs transfected with AAV9 SERCA, LDH leakage was inhibited (Fig. 3A) and the number of TUNEL–positive cells was reduced (Fig. 3B and C), suggesting that SERCA could partially but significantly suppress I/R-mediated endothelial death.

To understand whether endothelial death induced by I/R injury is executed through necroptosis, apoptosis, or both, western blots were used to analyze markers of apoptosis or necroptosis. According to previous studies, necroptosis is caused by activation of the Ripk3/PGAM5 signaling pathway and a drop in ATP generation [25]. Upon H/R stimulation, both Ripk3 and PGAM5 expression started to accumulate in CMECs (Fig. 3D–F) relative to the baseline. In addition, the total intracellular ATP content was downregulated in H/R-treated CMECs relative to the control group (Fig. 3G). By comparison, SERCA overexpression prevented ATP reduction and inhibited Ripk3/PGAM5 accumulation (Fig. 3D–G). Like necroptosis, apoptosis is a regulated cell death program governed by members of the caspase family, such as caspase-12, caspase-9, and caspase-3. Upon H/R injury, the activities of caspase-12, caspase-9, and caspase-12 increased rapidly, and this alteration could be repressed by SERCA (Fig. 3H–J). Taken together, our data highlight the existence of necroptosis and apoptosis in the development of cardiac microvascular I/R injury; both necroptosis and apoptosis could be repressed by SERCA overexpression.

3.4. Necroptosis is repressed by SERCA through the prevention of calcium overload, MCU activation, and mPTP opening

In light of the important role played by SERCA in regulating calcium homeostasis through timely and effectively reabsorption of intracellular calcium into the ER, we asked whether SERCA-deficiency–triggered necroptosis is correlated with intracellular calcium overload. Double-immunofluorescence of calcium staining detected a rise in intracellular calcium ($[Ca^{2+}]i$) and mitochondrial calcium ($[Ca^{2+}]m$) in H/R-treated CMECs over the control group (Fig. 4A–C). Interestingly, both $[Ca^{2+}]i$ and $[Ca^{2+}]m$ could be normalized by SERCA overexpression in CMECs in the presence of H/R injury (Fig. 4A–C). Although $[Ca^{2+}]m$ is affected by the concentration of $[Ca^{2+}]i$, the primary mediator of $[Ca^{2+}]m$ entry is the MCU, whose expression is correlated with the concentration of $[Ca^{2+}]m$ [56–58]. Of note, MCU expression was markedly elevated in H/R-treated cells and drastically lower in SERCA-overexpressed CMECs (Fig. 4D and E). These data indicate that SERCA regulates $[Ca^{2+}]m$ dependently on MCU.

Excessive calcium deposition is recognized as an initial step to inducing the opening of mPTP [59,60], a non-classical necroptotic signaling pathway, but this concept has not been verified in cardiac microvascular I/R injury. In comparison with the control group, the opening rate of mPTP was augmented approximately 3.3-fold by H/R injury and returned to baseline after transfection of AAV9 SERCA (Fig. 4F). Overall, SERCA overexpression significantly reduces $[Ca^{2+}]i/[Ca^{2+}]m$ overload, prevents MCU upregulation, and blocks mPTP opening; these beneficial actions may contribute to necroptosis inhibition in H/R-treated CMECs.

3.5. Induction of intracellular calcium overload or promotion of mitochondrial calcium entry induces endothelial cell necroptosis

To determine whether SERCA inhibits necroptosis through the calcium/MCU/mPTP pathway, $[Ca^{2+}]i$ activator (ionomycin) and MCU agonist (spermine) were administrated into SERCA-overexpressed

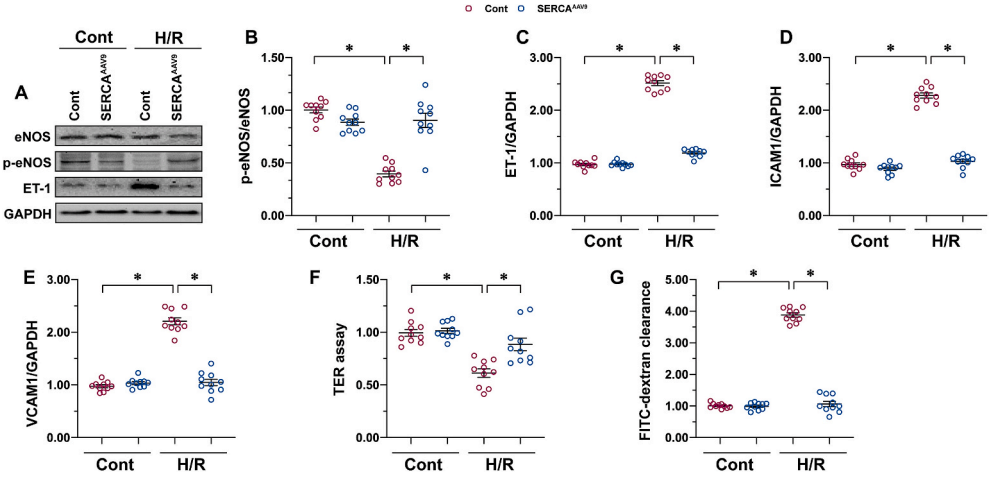

Fig. 2. SERCA overexpression improves endothelial function under H/R conditions. Primary CMECs were cultured in a vascular-cell basal medium supplemented with the endothelial cell growth kit VEGF. Hypoxia/reoxygenation (H/R) injury was induced through 30 min of hypoxia and 2 h of reoxygenation. SERCA AAV9 or control AAV9 vectors were transfected into CMECs, which were termed $SERCA^{AAV9}$ group or control group respectively. **A–C.** Proteins were isolated from H/R-treated CMECs, and then the levels of phosphorylated eNOS and ET-1 were measured through western blots. **D–E.** RNA was isolated from H/R-treated CMECs, and the transcriptions of ICAM1 and VCAM1 were determined through qPCR. **F–G.** Endothelial barrier function was determined through the FITC-dextran experiment and TER assay. *p < .05.

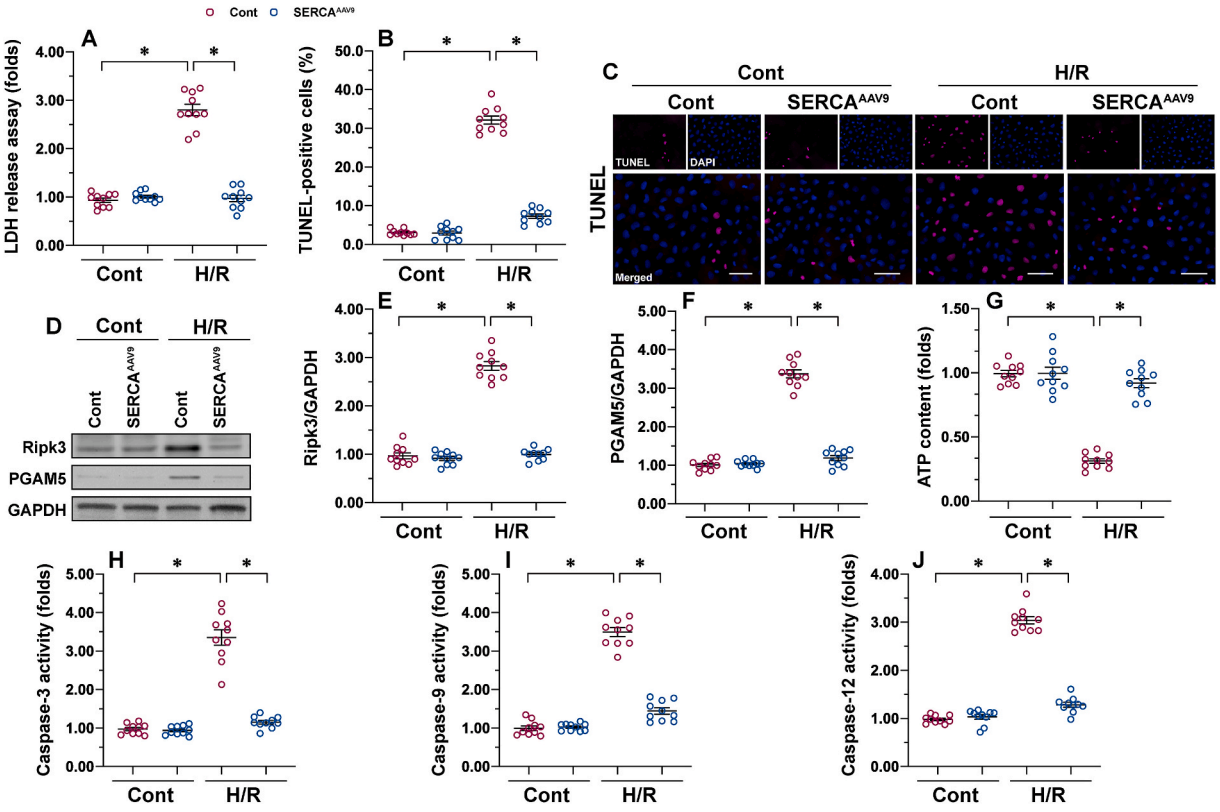

Fig. 3. Necroptosis and apoptosis can be reduced by SERCA. Primary CMECs were cultured in a vascular-cell basal medium supplemented with the endothelial cell growth kit VEGF. Hypoxia/reoxygenation (H/R) injury was induced through 30 min of hypoxia and 2 h of reoxygenation. SERCA AAV9 or control AAV9 vectors were transfected into CMECs, which were termed SERCA^{AAV9} group or control group respectively. **A.** Cell death was measured using the LDH cytotoxicity assay. **B–C.** TUNEL staining was used to observe the number of dead CMECs in response to H/R injury. **D–F.** Proteins were isolated from H/R-treated CMECs, and then the levels of Ripk3 and PGAM5 were measured using western blots. **G.** ATP production was measured using ELISA. **H–I.** Proteins were isolated from H/R-treated CMECs, and then the activities of caspase-3, caspase-12, and caspase-9 were evaluated. *p < .05.

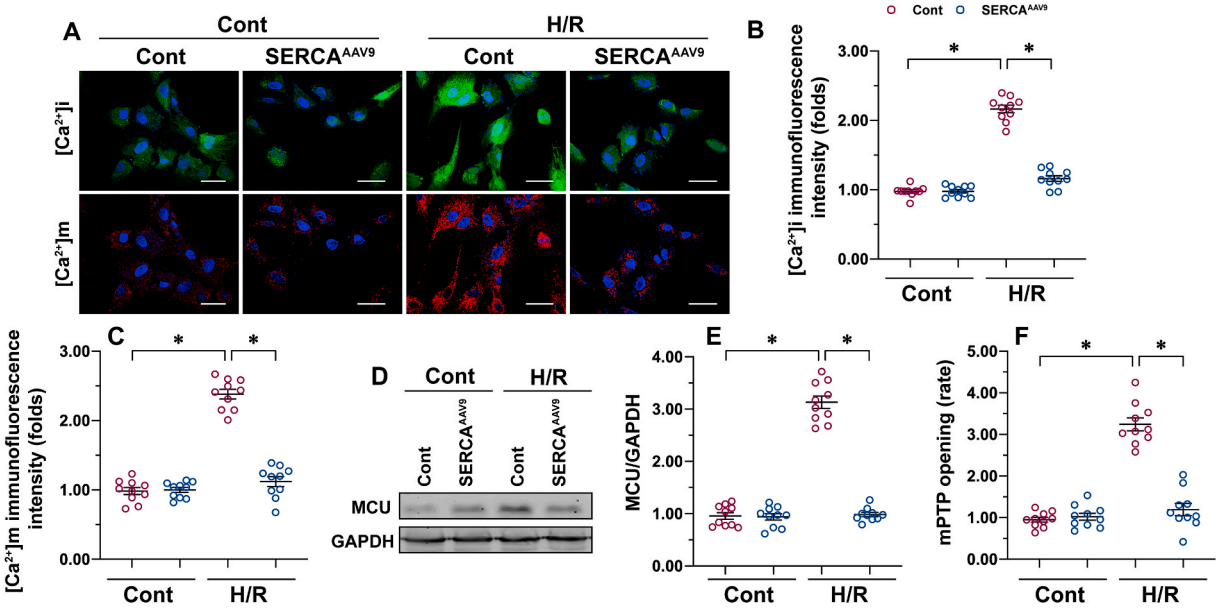

Fig. 4. Necroptosis is repressed by SERCA through the prevention of calcium overload, MCU activation, and mPTP opening. Primary CMECs were cultured in a vascular-cell basal medium supplemented with the endothelial cell growth kit VEGF. Hypoxia/reoxygenation (H/R) injury was induced through 30 min of hypoxia and 2 h of reoxygenation. SERCA AAV9 or control AAV9 vectors were transfected into CMECs, which were termed SERCA^{AAV9} group or control group respectively. **A–C.** Intracellular calcium ([Ca^{2+}]i) and mitochondrial calcium ([Ca^{2+}]m) were stained using Furo-2AM (Molecular Probes) and Rhod-2 (Molecular Probes), respectively. **D–E.** Proteins were isolated from H/R-treated CMECs, and then the levels of MCU were measured through western blots. **F.** mPTP opening was measured using the calcein AM probe. *p < .05.

CMECs to offset the regulatory effects of SERCA on calcium homeostasis and MCU inhibition. An LDH cytotoxicity assay demonstrated that SERCA overexpression reduced LDH leakage from CMECs into the medium, but such alteration was undetectable in CMECs pretreated with ionomycin or spermine (Fig. 5A). In addition, cell viability, as assessed by MTT assay, was downregulated in response to H/R injury (Fig. 5B). Although SERCA overexpression improved CMEC viability, this protective effect was offset by ionomycin or spermine (Fig. 5B). In accordance with these alterations, intracellular ATP production was reduced by H/R injury and returned to normal levels with SERCA overexpression (Fig. 5C). By contrast, either ionomycin or spermine treatment obviously repressed ATP generation in SERCA-overexpressed CMECs (Fig. 5C). Last, a Western blot was performed to analyze the alterations to necroptosis-related proteins. As we observed above, the expressions of Ripk3 and PGAM5 were upregulated by H/R injury (Fig. 5D–F). Overexpression of SERCA prevented Ripk3 and PGAM5 accumulation, but this effect was abolished by ionomycin or spermine (Fig. 5D–F). Therefore, these results suggest that the inhibitory action of SERCA on the calcium/MCU/mPTP pathway interrupts necroptosis in I/R-treated CMECs.

3.6. *Activation of the calcium/MCU/mPTP pathway abolishes SERCA-mediated endothelial protection in vivo*

Further supporting our *in vitro* findings, either ionomycin or spermine was administrated to mice before I/R injury. Then SERCA-mediated microvascular protection was monitored again. Consistently with our above observations, SERCA overexpression reduced luminal stenosis, vascular wall edema, or endothelial prolapse in mice subjected to I/R (Fig. 6A). Interestingly, AAV9 SERCA delivery failed to exert microvascular protection in mice pretreated with ionomycin or spermine (Fig. 6A). Similarly, eNOS phosphorylation was normalized, whereas ET1 expression was repressed by SERCA overexpression after cardiac I/R injury; these improvements were not seen in mice treated with ionomycin or spermine (Fig. 6B–D). In addition, the transcription of inflammation cytokines was downregulated by SERCA overexpression in I/R-treated mice; these effects were abolished by ionomycin or spermine (Fig. 6E and F). These data confirm that SERCA-mediated microvascular protection works through a mechanism of inhibiting the calcium/MCU/mPTP pathway.

4. Discussion

Myocardial infarction is a result of decreased blood flow to the myocardium [3]. It is generally accepted that the reintroduction of fresh blood to the ischemic tissues is the most effective way to reduce ischemia-triggered cardiomyocyte damage or death [3,61]. However, post-ischemic reperfusion sensitizes cells to death through various mechanisms, including oxidative stress, calcium overload, ATP depletion, and inflammation response [62,63]. Therefore, clinical management of I/R injury is an important step to augmenting the benefits of reperfusion therapies to patients [64]. In comparison with cardiomyocytes, microvascular I/R injury is a neglected topic in the study of cardiac I/R injury because little attention has been paid to the molecular details of reperfusion-mediated endothelial dysfunction. However, many careful epidemiological studies have highlighted the functional significance of microvascular damage, which has been identified as an independent risk factor that predicts in-hospital mortality and one-year major adverse cardiovascular events [65]. Thereby, it is of the utmost importance to understand the pathological responses of

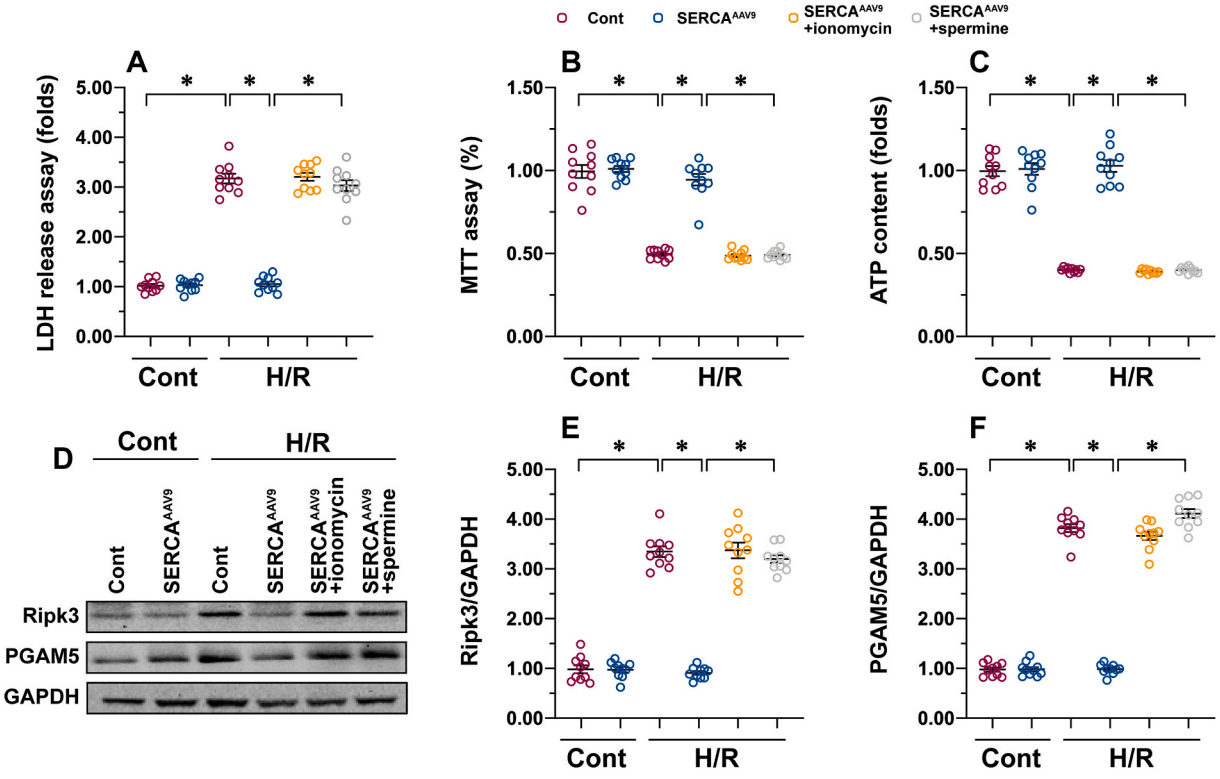

Fig. 5. Induction of intracellular calcium overload or promotion of mitochondrial calcium entry induces endothelial cell necroptosis. Primary CMECs were cultured in a vascular-cell basal medium supplemented with the endothelial cell growth kit VEGF. Hypoxia/reoxygenation (H/R) injury was induced through 30 min of hypoxia and 2 h of reoxygenation. SERCA AAV9 or control AAV9 vectors were transfected into CMECs, which were termed SERCA^{AAV9} group or control group respectively. [Ca^{2+}]i activator (ionomycin, 3 μM for 2 h) and MCU agonist (spermine, 10 μM for 2 h) were administrated into SERCA-overexpressed CMECs to offset the regulatory effects of SERCA on calcium homeostasis and MCU inhibition. **A.** Cell death was measured using the LDH cytotoxicity assay. **B.** An MTT assay was used to observe the viability of CMECs in response to H/R injury. **C.** ATP production was measured using ELISA. **D–F.** Proteins were isolated from H/R-treated CMECs, and then the levels of Ripk3 and PGAM5 were measured through western blots. *p < .05.

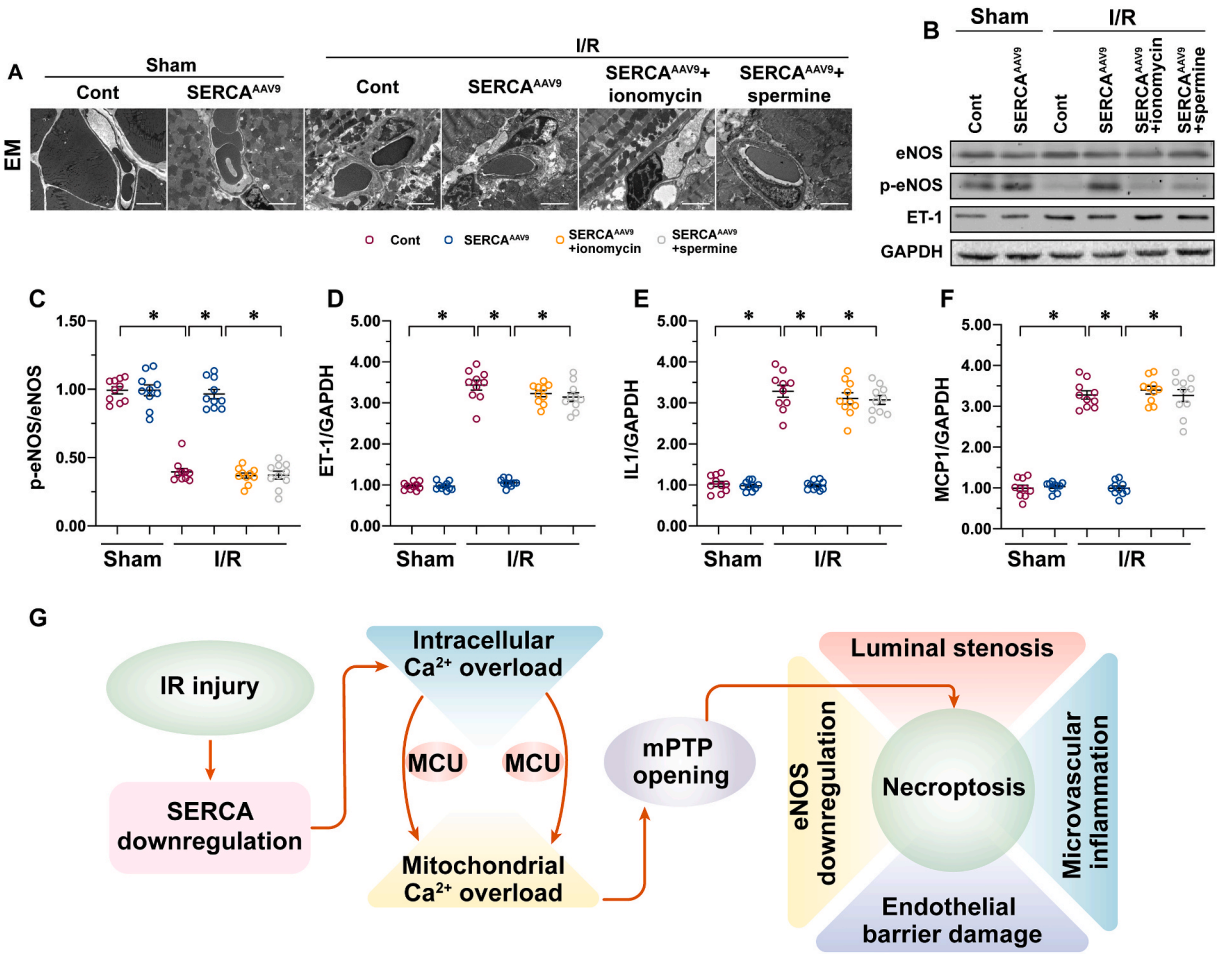

Fig. 6. Activation of the calcium/MCU/mPTP pathway abolishes SERCA-mediated endothelial protection *in vivo*. C57BL/6J mice received AAV9 SERCA (SERCA^{AAV9} group) or control AAV9 vectors (control group) before I/R injury. An I/R injury model was induced through 45 min of ischemia and 4 h of reperfusion. Animals in the sham group underwent all surgical procedures for I/R induction except the ligation step. To induce intracellular calcium overload, a single intraperitoneal (i.p.) injection of ionomycin at 1 mg/kg was given 30 min before the I/R model. In addition, to activate MCU in SERCA^{AAV9} mice, spermine i.p. treatment at 5 mg/kg was given 60 min before I/R surgery. **A.** Cardiac microcirculation was observed using an electron microscope (EM). **B–D.** Proteins were isolated from reperfused hearts, and then the levels of phosphorylated eNOS and ET-1 were measured through western blots. **E–F.** RNA was isolated from reperfused hearts, and the transcriptions of MCP1 and IL-1 were determined through qPCR. **G.** A schematic summary of our findings. Overexpression of SERCA attenuates the burden of intracellular calcium and thus inhibits MCU activation, resulting in the closure of mPTP and necroptosis inhibition. *p < .05.

endothelial cells to cardiac I/R injury.

In the present study, we found that endothelial cell death due to SERCA-deficiency–mediated necroptosis is the fundamental difficulty for microvascular functional maintenance during a post-ischemic reperfusion attack. Overexpression of SERCA attenuates the burden of intracellular calcium and thus inhibits MCU activation, resulting in the closing of mPTP and in necroptosis inhibition (Fig. 6G). This demonstrates that SERCA overexpression precisely confers resistance to microvascular damage in the post-ischemic heart. In addition, modifying SERCA activity, expression, or inhibition of the calcium/MCU/mPTP pathways would be the ideal approach to protecting cardiac microcirculation against I/R injury.

SERCA is a calcium pump that transports intracellular calcium to the ER [21,22]. The activity and expression of SERCA are vital for sustaining the baseline or resting intracellular calcium. Several studies have reported cardioprotective effects of SERCA [66]. For example, cardiomyocyte repolarization and contractility are handled by SERCA in cardiomyocytes through the Kv channels [67]. Diabetes-induced cardiac remodeling and cardiomyopathy are also linked to dysregulated SERCA in a manner dependent on the miR-133a [68]. A recent study reported a novel role for SERCA in preventing hypoxia-related cardiac depression independently of calcium regulation [69]. Of note, SERCA also plays an important role in regulating calcium homeostasis in non-cardiomyocytes cells, such as human embryonic stem cells [70]. In the present study, we found that endothelial calcium overload is also under the control of SERCA. I/R injury causes a drop in the expression of SERCA and thus promotes [Ca^{2+}]i/[Ca^{2+}]m overload. This finding may explain the vasospasm or the micro-vessel stenosis observed in reperfused heart tissue using EM. Our data provide evidence for the use of the calcium-channel regulator before or during reperfusion injury to reduce microvascular damage; this recommendation needs further verification in clinical practice.

Reperfusion injury is characterized by a loss of functional cells to apoptosis, necroptosis, and necrosis [71,72]. Unlike necrosis, apoptosis and necroptosis are programmed cell deaths that can be interrupted or blocked. Two biophysical and biochemical processes contribute to apoptosis and necroptosis activation during reperfusion injury: calcium overload and oxidative stress [32,71,73]. Cardiomyocytes have a pronounced susceptibility to calcium-mediated death regardless of apoptosis and necroptosis. Although necroptosis in the endothelium has been widely reported [74,75], the molecular network and signaling transduction of endothelial necroptosis have not been fully explained. In the present study, our data showed that dysregulated calcium due to SERCA downregulation is an early sign of necroptosis induction and

activation. Increased intracellular calcium triggers the opening of mPTP, and augmented mPTP opening has been reported to induce and transmit necroptotic signals through the promotion of mitochondrial rupture and mitochondrial ATP depletion [25]. Our data also highlight the regulatory effects of SERCA on Ripk3 and PGAM5, although the working mechanism has not been investigated. SERCA-regulated calcium balance may have an impact on Ripk3/PGAM5 activation, as a previous study showed a close relationship between calcium overload and Ripk3 upregulation [76]. Further experiments are needed to verify this hypothesis.

Overall, SERCA confers microvascular protection during cardiac I/R injury. Mechanically, overexpression of SERCA normalizes intracellular calcium signals and thus blocks calcium-triggered endothelial necroptosis, presumably driven by an inhibition of the calcium/MCU/mPTP pathways. This has important implications for the prevention of cardiac microvascular I/R injury.

Funding

This study is supported by Medical Research Project of Foshan Municipal Commission of Health and Family Planning (No: 20180099), Key Specialist Department Training Project of Foshan City, Guangdong Province of China (No: Fspy3-2015020), Key Medical Specialist Construction Project of Foshan during the 13th Five-Year Plan Period (No: FSZDZK135027).

Declaration of competing interest

The authors declare that they have no conflict of interest.

Acknowledgement

None.

References

[1] G. Heusch, 25 years of remote ischemic conditioning: from laboratory curiosity to clinical outcome, Basic Res. Cardiol. 113 (3) (2018) 15.
[2] S.M. Davidson, S. Arjun, M.V. Basalay, R.M. Bell, D.I. Bromage, H.E. Botker, R. D. Carr, J. Cunningham, A.K. Ghosh, G. Heusch, B. Ibanez, P. Kleinbongard, S. Lecour, H. Maddock, M. Ovize, M. Walker, M. Wiart, D.M. Yellon, The 10th Biennial Hatter Cardiovascular Institute workshop: cellular protection-evaluating new directions in the setting of myocardial infarction, ischaemic stroke, and cardio-oncology, Basic Res. Cardiol. 113 (6) (2018) 43.
[3] N. Hadebe, M. Cour, S. Lecour, The SAFE pathway for cardioprotection: is this a promising target? Basic Res. Cardiol. 113 (2) (2018) 9.
[4] G. Amanakis, P. Kleinbongard, G. Heusch, A. Skyschally, Attenuation of ST-segment elevation after ischemic conditioning maneuvers reflects cardioprotection online, Basic Res. Cardiol. 114 (3) (2019) 22.
[5] H.E. Botker, D. Hausenloy, I. Andreadou, S. Antonucci, K. Boengler, S.M. Davidson, S. Deshwal, Y. Devaux, F. Di Lisa, M. Di Sante, P. Efentakis, S. Femmino, D. Garcia-Dorado, Z. Giricz, B. Ibanez, E. Iliodromitis, N. Kaludercic, P. Kleinbongard, M. Neuhauser, M. Ovize, P. Pagliaro, M. Rahbek-Schmidt, M. Ruiz-Meana, K. D. Schluter, R. Schulz, A. Skyschally, C. Wilder, D.M. Yellon, P. Ferdinandy, G. Heusch, Practical guidelines for rigor and reproducibility in preclinical and clinical studies on cardioprotection, Basic Res. Cardiol. 113 (5) (2018) 39.
[6] G. Heusch, Coronary microvascular obstruction: the new frontier in cardioprotection, Basic Res. Cardiol. 114 (6) (2019) 45.
[7] P. Kleinbongard, A. Skyschally, S. Gent, M. Pesch, G. Heusch, STAT3 as a common signal of ischemic conditioning: a lesson on "rigor and reproducibility" in preclinical studies on cardioprotection, Basic Res. Cardiol. 113 (1) (2018) 3.
[8] T. Honda, Q. He, F. Wang, A.N. Redington, Acute and chronic remote ischemic conditioning attenuate septic cardiomyopathy, improve cardiac output, protect systemic organs, and improve mortality in a lipopolysaccharide-induced sepsis model, Basic Res. Cardiol. 114 (3) (2019) 15.
[9] J.T. Opferman, A. Kothari, Anti-apoptotic BCL-2 family members in development, Cell Death Differ. 25 (1) (2018) 37–45.
[10] M. Someda, S. Kuroki, H. Miyachi, M. Tachibana, S. Yonehara, Caspase-8, receptor-interacting protein kinase 1 (RIPK1), and RIPK3 regulate retinoic acid-induced cell differentiation and necroptosis, Cell Death Differ. 27 (5) (2019) 1539–1553.
[11] Y. Xiong, L. Li, L. Zhang, Y. Cui, C. Wu, H. Li, K. Chen, Q. Yang, R. Xiang, Y. Hu, S. Huang, Y. Wei, S. Yang, The bromodomain protein BRD4 positively regulates necroptosis via modulating MLKL expression, Cell Death Differ. 26 (10) (2019) 1929–1941.
[12] L. Bacmeister, M. Schwarzl, S. Warnke, B. Stoffers, S. Blankenberg, D. Westermann, D. Lindner, Inflammation and fibrosis in murine models of heart failure, Basic Res. Cardiol. 114 (3) (2019) 19.
[13] J. Beckendorf, M.M.G. Van Den Hoogenhof, J. Backs, Physiological and unappreciated roles of CaMKII in the heart, Basic Res. Cardiol. 113 (4) (2018) 29.
[14] J. Wang, S. Toan, H. Zhou, New insights into the role of mitochondria in cardiac microvascular ischemia/reperfusion injury, Angiogenesis 23 (3) (2020) 299–314.
[15] J. Wang, S. Toan, H. Zhou, Mitochondrial quality control in cardiac microvascular ischemia-reperfusion injury: new insights into the mechanisms and therapeutic potentials, Pharmacol. Res. 156 (2020) 104771.
[16] J. Gambardella, B. Trimarco, G. Iaccarino, G. Santulli, New insights in cardiac calcium handling and excitation-contraction coupling, Adv. Exp. Med. Biol. 1067 (2018) 373–385.
[17] F. Abi-Samra, D. Gutterman, Cardiac contractility modulation: a novel approach for the treatment of heart failure, Heart Fail. Rev. 21 (6) (2016) 645–660.
[18] Y. Zhang, H. Zhou, W. Wu, C. Shi, S. Hu, T. Yin, Q. Ma, T. Han, Y. Zhang, F. Tian, Y. Chen, Liraglutide protects cardiac microvascular endothelial cells against hypoxia/reoxygenation injury through the suppression of the SR-Ca(2+)-XO-ROS axis via activation of the GLP-1R/PI3K/Akt/survivin pathways, Free Radic. Biol. Med. 95 (2016) 278–292.
[19] J. Guo, Y. Bian, R. Bai, H. Li, M. Fu, C. Xiao, Globular adiponectin attenuates myocardial ischemia/reperfusion injury by upregulating endoplasmic reticulum Ca (2)(+)-ATPase activity and inhibiting endoplasmic reticulum stress, J. Cardiovasc. Pharmacol. 62 (2) (2013) 143–153.
[20] N. Hiranandani, T. Bupha-Intr, P.M. Janssen, SERCA overexpression reduces hydroxyl radical injury in murine myocardium, Am. J. Physiol. Heart Circ. Physiol. 291 (6) (2006) H3130–H3135.
[21] S. Zhang, W. Wang, X. Wu, X. Zhou, Regulatory roles of circular RNAs in coronary artery disease, Mol. Ther. Nucleic Acids 21 (2020) 172–179.
[22] G. Hasenfuss, J.R. Teerlink, Cardiac inotropes: current agents and future directions, Eur. Heart J. 32 (15) (2011) 1838–1845.
[23] H. Zhu, Q. Jin, Y. Li, Q. Ma, J. Wang, D. Li, H. Zhou, Y. Chen, Melatonin protected cardiac microvascular endothelial cells against oxidative stress injury via suppression of IP3R-[Ca(2+)]c/VDAC-[Ca(2+)]m axis by activation of MAPK/ERK signaling pathway, Cell Stress Chaperones 23 (1) (2018) 101–113.
[24] H. Zhou, S. Toan, Pathological roles of mitochondrial oxidative stress and mitochondrial dynamics in cardiac microvascular ischemia/reperfusion injury, Biomolecules 10 (1) (2020).
[25] H. Zhou, D. Li, P. Zhu, Q. Ma, S. Toan, J. Wang, S. Hu, Y. Chen, Y. Zhang, Inhibitory effect of melatonin on necroptosis via repressing the Ripk3-PGAM5-CypD-mPTP pathway attenuates cardiac microvascular ischemia-reperfusion injury, J. Pineal Res. 65 (3) (2018), e12503.
[26] P. Zhu, S. Hu, Q. Jin, D. Li, F. Tian, S. Toan, Y. Li, H. Zhou, Y. Chen, Ripk3 promotes ER stress-induced necroptosis in cardiac IR injury: a mechanism involving calcium overload/XO/ROS/mPTP pathway, Redox Biol 16 (2018) 157–168.
[27] B.W.L. Lee, P. Ghode, D.S.T. Ong, Redox regulation of cell state and fate, Redox Biol 25 (2019) 101056.
[28] D. Li, X. Wang, Q. Huang, S. Li, Y. Zhou, Z. Li, Cardioprotection of CAPE-oNO2 against myocardial ischemia/reperfusion induced ROS generation via regulating the SIRT1/eNOS/NF-kappaB pathway in vivo and in vitro, Redox Biol 15 (2018) 62–73.
[29] T. Frank, M. Tuppi, M. Hugle, V. Dotsch, S.J.L. Van Wijk, S. Fulda, Cell cycle arrest in mitosis promotes interferon-induced necroptosis, Cell Death Differ. 26 (10) (2019) 2046–2060.
[30] P.K. Singh, A. Roukounakis, A. Weber, K.K. Das, B. Sohm, A. Villunger, A.J. Garcia-Saez, G. Hacker, Dynein light chain binding determines complex formation and posttranslational stability of the Bcl-2 family members Bmf and Bim, Cell Death Differ. (2019).
[31] L. Galluzzi, I. Vitale, S.A. Aaronson, J.M. Abrams, D. Adam, P. Agostinis, E. S. Alnemri, L. Altucci, I. Amelio, D.W. Andrews, M. Annicchiarico-Petruzzelli, A. V. Antonov, E. Arama, E.H. Baehrecke, N.A. Barlev, N.G. Bazan, F. Bernassola, M.J. M. Bertrand, K. Bianchi, M.V. Blagosklonny, K. Blomgren, C. Borner, P. Boya, C. Brenner, M. Campanella, E. Candi, D. Carmona-Gutierrez, F.K. Cecconi, F.K. Chan, N.S. Chandel, E.H. Cheng, J.E. Chipuk, J.A. Cidlowski, A. Ciechanover, G. M. Cohen, M. Conrad, J.R. Cubillos-Ruiz, P.E. Czabotar, V. D'angiolella, T. M. Dawson, V.L. Dawson, V. De Laurenzi, R. De Maria, K.M. Debatin, R. J. Deberardinis, M. Deshmukh, N. Di Daniele, F. Di Virgilio, V.M. Dixit, S.J. Dixon, C.S. Duckett, B.D. Dynlacht, W.S. El-Deiry, J.W. Elrod, G.M. Fimia, S. Fulda, A. J. Garcia-Saez, A.D. Garg, C. Garrido, E. Gavathiotis, P. Golstein, E. Gottlieb, D. R. Green, L.A. Greene, H. Gronemeyer, A. Gross, G. Hajnoczky, J.M. Hardwick, I. S. Harris, M.O. Hengartner, C. Hetz, H. Ichijo, M. Jaattela, B. Joseph, P.J. Jost, P. P. Juin, W.J. Kaiser, M. Karin, T. Kaufmann, O. Kepp, A. Kimchi, R.N. Kitsis, D. J. Klionsky, R.A. Knight, S. Kumar, S.W. Lee, J.J. Lemasters, B. Levine, A. Linkermann, S.A. Lipton, R.A. Lockshin, C. Lopez-Otin, S.W. Lowe, T. Luedde, E. Lugli, M. Macfarlane, F. Madeo, M. Malewicz, W. Malorni, G. Manic, J. C. Marine, S.J. Martin, J.C. Martinou, J.P. Medema, P. Mehlen, P. Meier, S. Melino, E.A. Miao, J.D. Molkentin, U.M. Moll, C. Munoz-Pinedo, S. Nagata, G. Nunez, A. Oberst, M. Oren, M. Overholtzer, M. Pagano, T. Panaretakis, M. Pasparakis, J. M. Penninger, D.M. Pereira, S. Pervaiz, M.E. Peter, M. Piacentini, P. Pinton, J.H. M. Prehn, H. Puthalakath, G.A. Rabinovich, M. Rehm, R. Rizzuto, C.M. P. Rodrigues, D.C. Rubinsztein, T. Rudel, K.M. Ryan, E. Sayan, L. Scorrano, F. Shao, Y. Shi, J. Silke, H.U. Simon, A. Sistigu, B.R. Stockwell, A. Strasser, G. Szabadkai, S. W.G. Tait, D. Tang, N. Tavernarakis, A. Thorburn, Y. Tsujimoto, B. Turk, T. Vanden Berghe, P. Vandenabeele, M.G. Vander Heiden, A. Villunger, H.W. Virgin, K. H. Vousden, D. Vucic, E.F. Wagner, H. Walczak, D. Wallach, Y. Wang, J.A. Wells,

W. Wood, J. Yuan, Z. Zakeri, B. Zhivotovsky, L. Zitvogel, G. Melino, G. Kroemer, Molecular mechanisms of cell death: recommendations of the nomenclature committee on cell death, Cell Death Differ. 25 (3) (2018) 486–541, 2018.
[32] D.P. Del Re, D. Amgalan, A. Linkermann, Q. Liu, R.N. Kitsis, Fundamental mechanisms of regulated cell death and implications for heart disease, Physiol. Rev. 99 (4) (2019) 1765–1817.
[33] R.L. Quispe, M.L. Jaramillo, L.S. Galant, D. Engel, A.L. Dafre, J.B. Teixeira Da Rocha, R. Radi, M. Farina, A.F. De Bem, Diphenyl diselenide protects neuronal cells against oxidative stress and mitochondrial dysfunction: involvement of the glutathione-dependent antioxidant system, Redox Biol 20 (2019) 118–129.
[34] T. Zhang, Y. Zhang, M. Cui, L. Jin, Y. Wang, F. Lv, Y. Liu, W. Zheng, H. Shang, J. Zhang, M. Zhang, H. Wu, J. Guo, X. Zhang, X. Hu, C.M. Cao, R.P. Xiao, CaMKII is a RIP3 substrate mediating ischemia- and oxidative stress-induced myocardial necroptosis, Nat. Med. 22 (2) (2016) 175–182.
[35] B.L. Heckmann, B. Tummers, D.R. Green, Crashing the computer: apoptosis vs. necroptosis in neuroinflammation, Cell Death Differ. 26 (1) (2019) 41–52.
[36] M.D. Stutz, S. Ojaimi, C. Allison, S. Preston, P. Arandjelovic, J.M. Hildebrand, J. J. Sandow, A.I. Webb, J. Silke, W.S. Alexander, M. Pellegrini, Necroptotic signaling is primed in Mycobacterium tuberculosis-infected macrophages, but its pathophysiological consequence in disease is restricted, Cell Death Differ. 25 (5) (2018) 951–965.
[37] E.H. Kim, S.W. Wong, J. Martinez, Programmed Necrosis and Disease:We interrupt your regular programming to bring you necroinflammation, Cell Death Differ. 26 (1) (2019) 25–40.
[38] H. Zhou, P. Zhu, J. Wang, H. Zhu, J. Ren, Y. Chen, Pathogenesis of cardiac ischemia reperfusion injury is associated with CK2alpha-disturbed mitochondrial homeostasis via suppression of FUNDC1-related mitophagy, Cell Death Differ. 25 (6) (2018) 1080–1093.
[39] H. Zhou, J. Wang, P. Zhu, H. Zhu, S. Toan, S. Hu, J. Ren, Y. Chen, NR4A1 aggravates the cardiac microvascular ischemia reperfusion injury through suppressing FUNDC1-mediated mitophagy and promoting Mff-required mitochondrial fission by CK2alpha, Basic Res. Cardiol. 113 (4) (2018) 23.
[40] S. Li, H.X. Xu, C.T. Wu, W.Q. Wang, W. Jin, H.L. Gao, H. Li, S.R. Zhang, J.Z. Xu, Z. H. Qi, Q.X. Ni, X.J. Yu, L. Liu, Angiogenesis in pancreatic cancer: current research status and clinical implications, Angiogenesis 22 (1) (2019) 15–36.
[41] S. Guo, J. Lu, Y. Zhuo, M. Xiao, X. Xue, S. Zhong, X. Shen, C. Yin, L. Li, Q. Chen, M. Zhu, B. Chen, M. Zhao, L. Zheng, Y. Tao, H. Yin, Endogenous cholesterol ester hydroperoxides modulate cholesterol levels and inhibit cholesterol uptake in hepatocytes and macrophages, Redox Biol 21 (2019) 101069.
[42] H. Zhou, C. Shi, S. Hu, H. Zhu, J. Ren, Y. Chen, BI1 is associated with microvascular protection in cardiac ischemia reperfusion injury via repressing Syk-Nox2-Drp1-mitochondrial fission pathways, Angiogenesis 21 (3) (2018) 599–615.
[43] S. Man, G. Sanchez Duffhues, P. Ten Dijke, D. Baker, The therapeutic potential of targeting the endothelial-to-mesenchymal transition, Angiogenesis 22 (1) (2019) 3–13.
[44] A. Graczyk-Jarzynka, A. Goral, A. Muchowicz, R. Zagozdzon, M. Winiarska, M. Bajor, A. Trzeciecka, K. Fidyt, J.A. Krupka, J. Cyran, K. Szczygiel, D.G. Efremov, S. Gobessi, A. Jagielski, K. Siudakowska, M. Bobrowicz, M. Klopotowska, J. Barankiewicz, A. Malenda, E. Lech-Maranda, N. Miazek-Zapala, P.H. Skarzynski, A. Domagala, J. Golab, M. Firczuk, Inhibition of thioredoxin-dependent H2O2 removal sensitizes malignant B-cells to pharmacological ascorbate, Redox Biol 21 (2019) 101062.
[45] Z.G. Ma, J. Dai, Y.P. Yuan, Z.Y. Bian, S.C. Xu, Y.G. Jin, X. Zhang, Q.Z. Tang, T-bet deficiency attenuates cardiac remodelling in rats, Basic Res. Cardiol. 113 (3) (2018) 19.
[46] J. Li, X. Yan, J. Tang, Y. Wang, J. Tang, W. Wu, M. Liu, HDAC2-mediated upregulation of IL-6 triggers the migration of osteosarcoma cells, Cell Biol. Toxicol. 35 (5) (2019) 423–433.
[47] H.C. Chang, C.H. Kao, S.Y. Chung, W.C. Chen, L.P. Aninda, Y.H. Chen, Y.A. Juan, S. L. Chen, Bhlhe40 differentially regulates the function and number of peroxisomes and mitochondria in myogenic cells, Redox Biol 20 (2019) 321–333.
[48] M. Bocci, J. Sjolund, E. Kurzejamska, D. Lindgren, N.A. Marzouka, M. Bartoschek, M. Hoglund, K. Pietras, Activin receptor-like kinase 1 is associated with immune cell infiltration and regulates CLEC14A transcription in cancer, Angiogenesis 22 (1) (2019) 117–131.
[49] M. Ikeda, Y. Ishima, R. Kinoshita, V.T.G. Chuang, N. Tasaka, N. Matsuo, H. Watanabe, T. Shimizu, T. Ishida, M. Otagiri, T. Maruyama, A novel S-sulfhydrated human serum albumin preparation suppresses melanin synthesis, Redox Biol 14 (2018) 354–360.
[50] L. Bramasole, A. Sinha, S. Gurevich, M. Radzinski, Y. Klein, N. Panat, E. Gefen, T. Rinaldi, D. Jimenez-Morales, J. Johnson, N.J. Krogan, N. Reis, D. Reichmann, M. H. Glickman, E. Pick, Proteasome lid bridges mitochondrial stress with Cdc53/Cullin1 NEDDylation status, Redox Biol 20 (2019) 533–543.
[51] C. Battistelli, G. Sabarese, L. Santangelo, C. Montaldo, F.J. Gonzalez, M. Tripodi, C. Cicchini, The lncRNA HOTAIR transcription is controlled by HNF4alpha-induced chromatin topology modulation, Cell Death Differ. 26 (5) (2019) 890–901.
[52] M. Bittremieux, R.M. La Rovere, H. Akl, C. Martines, K. Welkenhuyzen, K. Dubron, M. Baes, A. Janssens, P. Vandenberghe, L. Laurenti, K. Rietdorf, G. Morciano, P. Pinton, K. Mikoshiba, M.D. Bootman, D.G. Efremov, H. De Smedt, J.B. Parys, G. Bultynck, Constitutive IP3 signaling underlies the sensitivity of B-cell cancers to the Bcl-2/IP3 receptor disruptor BIRD-2, Cell Death Differ. 26 (3) (2019) 531–547.
[53] J.X. Sun, T.F. Chang, M.H. Li, L.J. Sun, X.C. Yan, Z.Y. Yang, Y. Liu, W.Q. Xu, Y. Lv, J.B. Su, L. Liang, H. Han, G.R. Dou, Y.S. Wang, SNAI1, an endothelial-mesenchymal transition transcription factor, promotes the early phase of ocular neovascularization, Angiogenesis 21 (3) (2018) 635–652.
[54] Q. Jin, R. Li, N. Hu, T. Xin, P. Zhu, S. Hu, S. Ma, H. Zhu, J. Ren, H. Zhou, DUSP1 alleviates cardiac ischemia/reperfusion injury by suppressing the Mff-required mitochondrial fission and Bnip3-related mitophagy via the JNK pathways, Redox Biol 14 (2018) 576–587.
[55] Y.R. Kim, J.I. Baek, S.H. Kim, M.A. Kim, B. Lee, N. Ryu, K.H. Kim, D.G. Choi, H. M. Kim, M.P. Murphy, G. Macpherson, Y.S. Choo, J. Bok, K.Y. Lee, J.W. Park, U. K. Kim, Therapeutic potential of the mitochondria-targeted antioxidant MitoQ in mitochondrial-ROS induced sensorineural hearing loss caused by Idh2 deficiency, Redox Biol 20 (2019) 544–555.
[56] L. Gu, J.L. Larson Casey, S.A. Andrabi, J.H. Lee, S. Meza-Perez, T.D. Randall, A. B. Carter, Mitochondrial calcium uniporter regulates PGC-1alpha expression to mediate metabolic reprogramming in pulmonary fibrosis, Redox Biol 26 (2019) 101307.
[57] L. Wu, J.L. Tan, Z.Y. Chen, G. Huang, Cardioprotection of post-ischemic moderate ROS against ischemia/reperfusion via STAT3-induced the inhibition of MCU opening, Basic Res. Cardiol. 114 (5) (2019) 39.
[58] G. Gherardi, L. Nogara, S. Ciciliot, G.P. Fadini, B. Blaauw, P. Braghetta, P. Bonaldo, D. De Stefani, R. Rizzuto, C. Mammucari, Loss of mitochondrial calcium uniporter rewires skeletal muscle metabolism and substrate preference, Cell Death Differ. 26 (2) (2019) 362–381.
[59] M.J. Perez, D.P. Ponce, A. Aranguiz, M.I. Behrens, R.A. Quintanilla, Mitochondrial permeability transition pore contributes to mitochondrial dysfunction in fibroblasts of patients with sporadic Alzheimer's disease, Redox Biol 19 (2018) 290–300.
[60] L. Maatouk, C. Yi, M.A. Carrillo-De Sauvage, A.C. Compagnion, S. Hunot, P. Ezan, E.C. Hirsch, A. Koulakoff, F.W. Pfrieger, F. Tronche, L. Leybaert, C. Giaume, S. Vyas, Glucocorticoid receptor in astrocytes regulates midbrain dopamine neurodegeneration through connexin hemichannel activity, Cell Death Differ. 26 (3) (2019) 580–596.
[61] J.P. Audia, X.M. Yang, E.S. Crockett, N. Housley, E.U. Haq, K. O'donnell, M. V. Cohen, J.M. Downey, D.F. Alvarez, Caspase-1 inhibition by VX-765 administered at reperfusion in P2Y12 receptor antagonist-treated rats provides long-term reduction in myocardial infarct size and preservation of ventricular function, Basic Res. Cardiol. 113 (5) (2018) 32.
[62] D. Curley, B. Lavin Plaza, A.M. Shah, R.M. Botnar, Molecular imaging of cardiac remodelling after myocardial infarction, Basic Res. Cardiol. 113 (2) (2018) 10.
[63] R.A. Eid, M.A. Alkhateeb, S. Eleawa, F.H. Al-Hashem, M. Al-Shraim, A.F. El-Kott, M.S.A. Zaki, M.A. Dallak, H. Aldera, Cardioprotective effect of ghrelin against myocardial infarction-induced left ventricular injury via inhibition of SOCS3 and activation of JAK2/STAT3 signaling, Basic Res. Cardiol. 113 (2) (2018) 13.
[64] A. Gaspar, A.P. Lourenco, M.A. Pereira, P. Azevedo, R. Roncon-Albuquerque Jr., J. Marques, A.F. Leite-Moreira, Randomized controlled trial of remote ischaemic conditioning in ST-elevation myocardial infarction as adjuvant to primary angioplasty (RIC-STEMI), Basic Res. Cardiol. 113 (3) (2018) 14.
[65] J. Zhong, H. Ouyang, M. Sun, J. Lu, Y. Zhong, Y. Tan, Y. Hu, Tanshinone IIA attenuates cardiac microvascular ischemia-reperfusion injury via regulating the SIRT1-PGC1alpha-mitochondrial apoptosis pathway, Cell Stress Chaperones 24 (5) (2019) 991–1003.
[66] E.G. Kranias, R.J. Hajjar, Modulation of cardiac contractility by the phospholamban/SERCA2a regulatome, Circ. Res. 110 (12) (2012) 1646–1660.
[67] F. Altamirano, G.G. Schiattarella, K.M. French, S.Y. Kim, F. Engelberger, S. Kyrychenko, E. Villalobos, D. Tong, J.W. Schneider, C.A. Ramirez-Sarmiento, S. Lavandero, T.G. Gillette, J.A. Hill, Polycystin-1 assembles with Kv channels to govern cardiomyocyte repolarization and contractility, Circulation 140 (11) (2019) 921–936.
[68] T.N. Kambis, H.R. Shahshahan, S. Kar, S.K. Yadav, P.K. Mishra, Transgenic expression of miR-133a in the diabetic akita heart prevents cardiac remodeling and cardiomyopathy, Front Cardiovasc Med 6 (2019) 45.
[69] A.L. Williams, C.B. Walton, K.A. Maccannell, A. Avelar, R.V. Shohet, HIF-1 regulation of miR-29c impairs SERCA2 expression and cardiac contractility, Am. J. Physiol. Heart Circ. Physiol. 316 (3) (2019) H554–H565.
[70] S. Li, A. Chopra, W. Keung, C.W.Y. Chan, K.D. Costa, C.W. Kong, R.J. Hajjar, C. S. Chen, R.A. Li, Sarco/endoplasmic reticulum Ca(2+)-ATPase is a more effective calcium remover than sodium-calcium exchanger in human embryonic stem cell-derived cardiomyocytes, Am. J. Physiol. Heart Circ. Physiol. 317 (5) (2019) H1105–H1115.
[71] H.M. Schmidt, E.E. Kelley, A.C. Straub, The impact of xanthine oxidase (XO) on hemolytic diseases, Redox Biol 21 (2019) 101072.
[72] A.J. Kowaltowski, Strategies to detect mitochondrial oxidants, Redox Biol 21 (2019) 101065.
[73] M.I. Oerlemans, S. Koudstaal, S.A. Chamuleau, D.P. De Kleijn, P.A. Doevendans, J. P. Sluijter, Targeting cell death in the reperfused heart: pharmacological approaches for cardioprotection, Int. J. Cardiol. 165 (3) (2013) 410–422.
[74] W. Huang, W. Xie, J. Gong, W. Wang, S. Cai, Q. Huang, Z. Chen, Y. Liu, Heat stress induces RIP1/RIP3-dependent necroptosis through the MAPK, NF-kappaB, and c-Jun signaling pathways in pulmonary vascular endothelial cells, Biochem. Biophys. Res. Commun. 528 (1) (2020) 206–212.
[75] J. Dai, C. Zhang, L. Guo, H. He, K. Jiang, Y. Huang, X. Zhang, H. Zhang, W. Wei, Y. Zhang, L. Lu, J. Hu, A necroptotic-independent function of MLKL in regulating endothelial cell adhesion molecule expression, Cell Death Dis. 11 (4) (2020) 282.
[76] H. Zhou, J. Wang, P. Zhu, S. Hu, J. Ren, Ripk3 regulates cardiac microvascular reperfusion injury: the role of IP3R-dependent calcium overload, XO-mediated oxidative stress and F-action/filopodia-based cellular migration, Cell. Signal. 45 (2018) 12–22.